

Published in final edited form as:

Biochemistry. 2013 January 15; 52(2): 279–281. doi:10.1021/bi301350s.

Simulation-based prediction of PIP₂ binding to an ion channel

Matthias R. Schmidt[†], Phillip J. Stansfeld[†], Stephen J. Tucker[‡], and Mark S. P. Sansom^{†,*}

[†]Department of Biochemistry, University of Oxford, Oxford OX1 3QU, United Kingdom

[‡]Clarendon Laboratory, Department of Physics, University of Oxford, Oxford OX1 3PU, United Kingdom

Abstract

Protein–lipid interactions regulate many membrane protein functions. Using a multi-scale approach which combines coarse-grained and atomistic molecular dynamics simulations we have predicted the binding site for the anionic phospholipid phosphatidylinositol 4,5-bisphosphate (PIP₂) on the Kir2.2 inwardly-rectifying (Kir) potassium channel. Comparison of the predicted binding site to that observed in the recent PIP₂-bound crystal structure of Kir2.2 reveals good agreement between simulation and experiment. In addition to providing insight into the mechanism by which PIP₂ binds to Kir2.2, these results help to establish the validity of this multi-scale simulation approach and its future application to examine novel membrane protein/lipid interactions in the increasing number of high-resolution membrane protein structures that are now available.

Lipid interactions with membrane proteins are an important component of many cell signaling pathways. The anionic lipid phosphatidylinositol 4,5-bisphosphate (PIP₂) plays a major role in such processes by acting as a secondary messenger, localizing proteins to membranes, and by regulating the activity of many different classes of ion channels¹. One of the effects of PIP₂ is the direct activation of inwardly-rectifying (Kir) potassium channels which modulate cellular electrical activity, and whose dysfunction underlies a wide range of inherited channelopathies^{2,3}. The binding site for PIP₂ in Kir channels was previously predicted using both conventional docking methods and simulation-based approaches⁴⁻⁶. However, these previous studies all employed homology models based upon the structure of a chimera between a eukaryotic and prokaryotic Kir channel in which several of the residues proposed to interact with PIP₂ were not fully resolved (PDB id 2QKS). Furthermore, this chimeric Kir/KirBac channel exhibits a complex functional interaction with PIP₂ and it is known that PIP₂ inhibits prokaryotic Kir channels^{7,8}. Consequently the accuracy of the binding site predicted in these original simulations remains uncertain.

*Corresponding Author: Phone: +44 1865 613306, mark.sansom@biochem.ox.ac.uk.

ASSOCIATED CONTENT

Supporting Information

Detailed methods, PIP₂ binding to an apo structure (PDB id 3SPI), electrostatic potential mapped on the PIP₂ binding site, simulations in a mixed bilayer, RMSF of the PIP₂ binding site. This material is available free of charge via the Internet at <http://pubs.acs.org>.

The authors declare no competing financial interests.

In this study, we have now taken advantage of several recently solved X-ray crystal structures of eukaryotic Kir channels to evaluate the binding site for PIP₂ in the Kir2.2 channel using a multi-scale molecular dynamics simulation approach⁵. This method employed coarse-grained (CG) simulations to predict initial PIP₂-binding events which were then refined by subsequent atomistic (AT) simulations⁹⁻¹³. In order to validate this prediction, the simulations were then compared to the crystal structures of Kir2.2 with either PIP₂ (PDB id 3SPI), or with the anionic lipid phosphatidic acid (PPA) bound (PDB id 3SPC). An apo-state structure without any bound lipid has also been solved (PDB id 3JYC)^{14, 15} and these different structures suggest an activation mechanism in which PIP₂ binding induces an upward translation and engagement of the C-terminal domain (CTD) with the transmembrane domain (TMD)¹⁴.

To explore the influence of these different initial conformations on these predictions as well as possible effects of the lipid bilayer, bound phospholipids were removed from the 3SPI and 3SPC Kir2.2 structures and both structures then used as input for multi-scale simulations of PIP₂ binding (Figure 1). To assess PIP₂ binding to a Kir2.2 apo-state, we also performed CG simulations using the 3JYC structure as input (Figure S1 of the Supporting Information). In addition to comparing our predicted binding sites with the PIP₂-bound 3SPI crystal structure, we also performed atomistic simulations of this PIP₂-bound structure. These reference simulations provide a more valid comparison with the multi-scale simulations, because it is then possible to directly compare simulations of both proteins embedded in a phospholipid bilayer at room temperature, rather than comparing a membrane-bound simulation with a static X-ray structure in the absence of a membrane.

Examination of the 3SPI crystal structure shows that residues which make contacts with the PIP₂ head group (Figure 1A) are mostly basic, and are either located on the N-terminal end of the first transmembrane helix TM1 (R78, W79, R80), or on the C-linker which connects the TMD with the CTD (K183, R186, K188, K189)¹⁴. We found that in the reference simulation of this structure all PIP₂-protein contacts were retained and accounted for nearly 90% of the total contacts made by side chains with the PIP₂ head groups (Figure 1B). Those residues which made less frequent contacts (~5%) with the PIP₂ head groups (K183, R186) were located on the C-linker. The C-linker is helical in the PIP₂-bound 3SPI structure, but flexible in other Kir2.2 crystal structures, and may therefore account for the differences observed for K183 and R186 in these simulations. However, the reference simulations appear to confirm the stability of the 3SPI structure and of the PIP₂-protein interactions in this structure.

Importantly, we found that the multi-scale simulations which used the protein coordinates from 3SPI as a starting structure predicted the PIP₂ head group to bind to the same cluster of basic residues as observed in the crystal structure (Figure 1C). This is in excellent agreement with both the reference simulations of this structure and with earlier predictions for other Kir channels^{5, 6}. Residues on TM1 (R78) and on the C-linker (K183, R186, K188, K189) were found to form the same number of contacts in the 3SPI multi-scale simulations as in the reference simulations (Figure 1B). Residue W79 on TM1 formed fewer contacts in the multi-scale simulations (5%) compared to the reference simulations (15%). The absence of any specific hydrogen bond interactions of W79 with PIP₂ in the crystal structure is likely to

render the orientation of this side chain more flexible and might be the reason for less frequent contacts between W79 and PIP₂ in the multi-scale simulations compared to the reference simulations. Although W79 is suggested to facilitate PIP₂ binding by anchoring TM1 at the membrane interface¹⁴, less frequent contacts argue against a direct interaction of W79 with PIP₂. The two adjacent residues (R80 and Y81) also exhibit differences between the multi-scale and reference simulations but this is most likely to be related to changes in TM2 which occur during the onset of channel gating. Nevertheless, these results demonstrate agreement between the PIP₂-bound 3SPI crystal structure, the 3SPI multi-scale simulations and the reference simulations.

In addition to using 3SPI, we also used the 3SPC protein coordinates as an input for the multi-scale predictions. This structure was crystallized with the anionic phospholipid PPA instead of PIP₂ and more closely resembles the apo-state structure (3JYC) in which the CTD is detached and not fully engaged with the TMD¹⁴. Strikingly, we found that when the ligand-free 3SPC structure was used as a starting point for the multi-scale simulations of PIP₂-binding, there was also good agreement between the multi-scale simulations and reference simulations (Figure 1D). Almost all contacts that were observed in the reference simulations were predicted by the 3SPC multi-scale simulations (Figure 1B) and were similar to those using 3SPI as a starting structure. The only major difference was the absence of any interaction between the head group of PIP₂ and R186 (Figure 1B). This is probably because in the 3SPC starting structure this 'C-linker' is less well ordered and the R186 side chain points in the opposite direction when compared to the PIP₂-bound 3SPI structure. Longer simulations may therefore be needed to see if R186 changes its orientation to interact with the PIP₂ head group.

Together these results clearly demonstrate that the multi-scale simulation approach can accurately predict the binding site for PIP₂ in Kir2.2 even when slightly different input structures are used. The principal advantage of the multi-scale approach compared to conventional docking methods is that both PIP₂ and the Kir2.2 channel are flexible. This can therefore provide insights into the molecular mechanisms underlying PIP₂ binding, such as conformational changes or an electrostatic contribution (Figure S2 of the Supporting Information), which more static docking approaches lack. Interestingly, during the simulations we observed that the phosphates of the PIP₂ head group formed transient hydrogen bonds with K220 on the CD loop. This resulted in a decrease of the C_α-C_α distance between K220 and a highly-conserved aspartate on the slide helix (D76) by 2–4 Å. This motion appears to be due to the CD loop moving upwards towards the slide helix and C-linker during PIP₂ binding, similar to the gating mechanism proposed in several other studies^{16, 17} and which may form part of a general activation mechanism for Kir channels by PIP₂⁶. Our results also suggest that PIP₂ binding to the C-linker stabilizes its α-helical structure, and may account for the interaction of PIP₂ with R186 in the 3SPI crystal structure. Moreover, using the multi-scale approach, the effect of the lipid bilayer composition on PIP₂ binding can be studied. Studies on liposomes of controlled lipid composition highlighted an anionic secondary lipid requirement for PIP₂-induced Kir channel activation¹⁸. We therefore repeated our CG simulations, replacing half of the lipids on the inner leaflet with the anionic phospholipid phosphatidylserine (PS), noting that PIP₂ still binds to Kir2.2, while PS, accumulating on either sides of the slide helix, distributes

unevenly around Kir2.2 (Figure S3 of the Supporting Information). This suggests a secondary binding site for anionic lipids in Kir channels.

In conclusion, these findings demonstrate good agreement between the PIP₂-bound crystal structure, the multi-scale predictions, and the reference simulations and therefore validate this multi-scale approach^{5, 6} for the prediction of PIP₂ binding sites. Consequently, this method may be confidently applied to the prediction of novel PIP₂ binding sites as well as the exploration of other lipid/channel interactions. For example, several eukaryotic voltage-gated potassium channels are regulated by PIP₂^{19, 20}, and enough high-resolution crystal structures now exist to enable similar multi-scale simulations of PIP₂ binding to these structures. Also, cholesterol has been shown to directly regulate Kir channel function but its precise binding site is unknown²¹. Many other unrelated ion channels and transporters, as well other classes of membrane proteins, have also been shown to be regulated by lipids²²⁻²⁴. Therefore, this multi-scale approach now provides an important and powerful tool to help study protein-lipid interactions and will become increasingly important with the ever expanding number of high-resolution membrane protein crystal structures now available.

Supplementary Material

Refer to Web version on PubMed Central for supplementary material.

ACKNOWLEDGMENT

We thank Dr Prafulla Aryal for most helpful comments on the manuscript.

Funding

This work was supported by the Engineering and Physical Sciences Research Council, Pfizer Neusentis, the Biotechnology and Biological Sciences Research Council, and the Wellcome Trust.

ABBREVIATIONS

PIP₂	phosphatidylinositol 4,5-bisphosphate
PPA	phosphatidic acid
PS	phosphatidylserine
Kir	inwardly rectifying potassium
K_v	voltage-gated potassium
TMD	transmembrane domain
CTD	C-terminal domain
CG	coarse-grained
AT	atomistic

REFERENCES

- (1). Suh BC, Hille B. Ann. Rev. Biophys. 2008; 37:175–195. [PubMed: 18573078]

- (2). Ashcroft FM. *Nature*. 2006; 440:440–447. [PubMed: 16554803]
- (3). Lopes CM, Zhang H, Rohacs T, Jin T, Yang J, Logothetis DE. *Neuron*. 2002; 34:933–944. [PubMed: 12086641]
- (4). Haider S, Tarasov AI, Craig TJ, Sansom MS, Ashcroft FM. *EMBO J*. 2007; 26:3749–3759. [PubMed: 17673911]
- (5). Stansfeld PJ, Hopkinson R, Ashcroft FM, Sansom MS. *Biochemistry*. 2009; 48:10926–10933. [PubMed: 19839652]
- (6). Meng X-Y, Zhang H-X, Logothetis DE, Cui M. *Biophys. J*. 2012; 102:2049–2059. [PubMed: 22824268]
- (7). Leal-Pinto E, Gómez-Llorente Y, Sundaram S, Tang Q-Y, Ivanova-Nikolova T, Mahajan R, Baki L, Zhang Z, Chavez J, Ubarretxena-Belandia I, Logothetis DE. *J. Biol. Chem*. 2010; 285:39790–39800. [PubMed: 20937804]
- (8). D’Avanzo N, Cheng WWL, Doyle DA, Nichols CG. *J. Biol. Chem*. 2010; 285:37129–37132. [PubMed: 20921230]
- (9). Stansfeld PJ, Sansom MSP. *J. Chem. Theory Comput*. 2011; 7:1157–1166.
- (10). Monticelli L, Kandasamy SK, Periole X, Larson RG, Tieleman DP, Marrink S-J. *J. Chem. Theory Comput*. 2008; 4:819–834.
- (11). Berger O, Edholm O, Jähnig F. *Biophys. J*. 1997; 72:2002–2013. [PubMed: 9129804]
- (12). Scott WRP, Hunenberger PH, Tironi IG, Mark AE, Billeter SR, Fennell J, Torda AE, Huber T, Kruger P, Van Gunsteren WF. *J. Phys. Chem. A*. 1999; 103:3596–3607.
- (13). Hess B, Kutzner C, Van der Spoel D, Lindahl E. *J. Chem. Theory Comput*. 2008; 4:435–447.
- (14). Hansen SB, Tao X, MacKinnon R. *Nature*. 2011; 477:495–498. [PubMed: 21874019]
- (15). Tao X, Avalos JL, Chen J, MacKinnon R. *Science*. 2009; 326:1668–1674. [PubMed: 20019282]
- (16). Whorton MR, MacKinnon R. *Cell*. 2011; 147:199–208. [PubMed: 21962516]
- (17). Bavro VN, De Zorzi R, Schmidt MR, Muniz JRC, Zubcevic L, Sansom MSP, Vénien-Bryan C, Tucker SJ. *Nat. Struct. Mol. Biol*. 2012; 19:158–163. [PubMed: 22231399]
- (18). Cheng WWL, D’Avanzo N, Doyle DA, Nichols CG. *Biophys. J*. 2011; 100:620–628. [PubMed: 21281576]
- (19). Rodriguez-Menchaca AA, Adney SK, Tang Q-Y, Meng X-Y, Rosenhouse-Dantsker A, Cui M, Logothetis DE. *Proc. Natl. Acad. Sci. USA*. 2012; 109:2399–2408.
- (20). Kruse M, Hammond GRV, Hille B. *J. Gen. Physiol*. 2012; 140:189–205. [PubMed: 22851677]
- (21). Rosenhouse-Dantsker A, Logothetis DE, Levitan I. *Biophys. J*. 2011; 100:381–389. [PubMed: 21244834]
- (22). Tucker SJ, Baukrowitz T. *J. Gen. Physiol*. 2008; 131:431–438. [PubMed: 18411329]
- (23). Coskun U, Simons K. *Structure*. 2011; 19:1543–1548. [PubMed: 22078554]
- (24). Aponte-Santamaría C, Briones R, Schenk AD, Walz T, De Groot BL. *Proc. Natl. Acad. Sci. USA*. 2012; 109:9887–9892. [PubMed: 22679286]

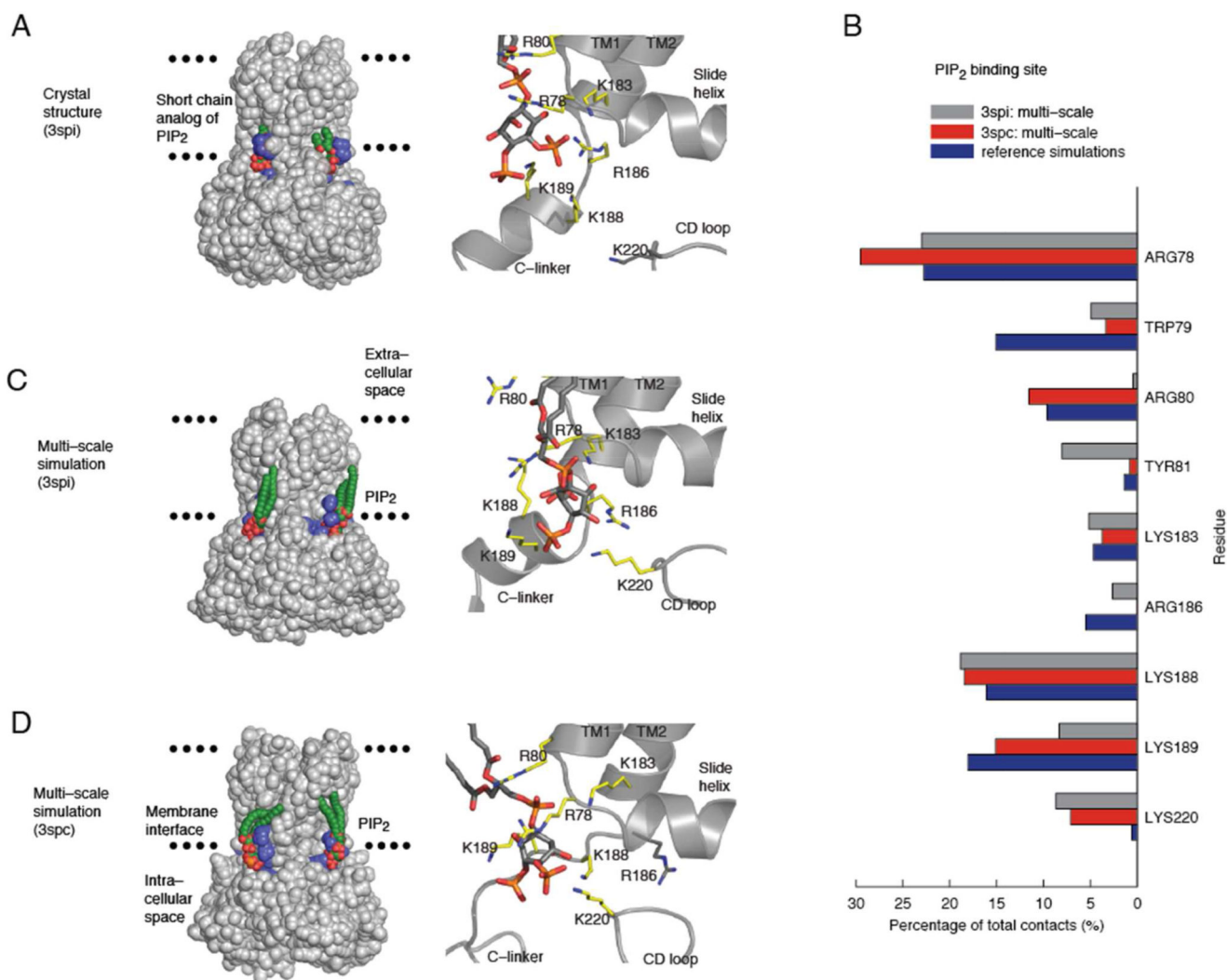


Figure 1. PIP₂ binding in Kir2.2 multi-scale simulations. A) Crystal structure with PIP₂ bound. For clarity, only two PIP₂ molecules are shown, with PIP₂-interacting residues in blue (left). Detailed view of the PIP₂ binding site (right) as found in the 3SPI structure. B) Multi-scale simulations used either 3SPI or 3SPC as starting structures and combined coarse-grained (CG; $24 \times 0.5 \mu\text{s}$) and atomistic (AT; $2 \times 0.1 \mu\text{s}$) simulations. Reference simulations were AT ($2 \times 0.1 \mu\text{s}$) of the PIP₂-bound 3SPI crystal structure. Residues whose side chains make more than 5% of the total contacts ($\approx 4\text{\AA}$) with PIP₂ head groups are compared between the multi-scale and reference simulations. C, D) The binding site of PIP₂ predicted by (C) 3SPI or (D) 3SPC multi-scale simulations. Parameters for PIP₂ can be found in the Supporting Information (Figure S4 and Table 1).